

Original Article

# Soft Synchronization of a Hydraulic Turbine Generator and Power Grid

Marcos Gabriel Saraza Mamani<sup>1</sup>, German Reymer Apaza Mayta<sup>1</sup>, German Alberto Echaiz Espinoza<sup>2</sup>, Pedro Alberto Mamani Apaza<sup>3</sup>, Fernando Enrique Echaiz Espinoza<sup>4</sup>

<sup>1</sup>Professional School of Electronic Engineering, Universidad Nacional de San Agustín de Arequipa, Arequipa, Perú.

<sup>2</sup>Academic Department of Electronic Engineering, Universidad Nacional de San Agustín de Arequipa, Arequipa, Perú.

<sup>3</sup>Academic Department of Mathematics, Universidad Nacional de San Agustín de Arequipa, Arequipa, Perú.

<sup>4</sup>Institute of Mathematics, Federal University of Alagoas, Alagoas, Brazil.

<sup>2</sup>Corresponding Author : [gechaiz@unsa.edu.pe](mailto:gechaiz@unsa.edu.pe)

Received: 04 March 2025

Revised: 09 April 2025

Accepted: 23 April 2025

Published: 31 May 2025

**Abstract** - This paper presents the analysis and simulation of synchronization between an active power grid and a power generation system driven by a Francis-type hydraulic turbine, using the model available in Simulink. Synchronization is a fundamental process in electrical systems, allowing the safe and efficient connection of generators in parallel with the grid. To achieve this, it is necessary to adjust the generator's voltage, frequency, and phase angle to match the grid values. Although physical equipment exists for this interconnection, this research simulates a soft synchronizer as an alternative to optimize the synchronization angle adjustment. To analyze the voltage signals, the d-q-0 reference frame transformation is employed, simplifying processing and enabling more precise detection of variations in voltage magnitude and phase angle. The theoretical framework of this research encompasses power system theory, electrical machines, and control, as well as mathematical models of Francis hydraulic turbines. Using Simulink libraries in MATLAB, the results obtained are evaluated based on variations in voltage, frequency, and phase angle during the transient synchronization period. The results show a considerable decrease in generator magnitude oscillations.

**Keywords** - Soft Synchronizer, Hydraulic Generator, Microgrid, Reference Frame Transformation, Signal Conditioner.

## 1. Introduction

A Microgrid (MG) is a system composed of Distributed Energy Resources (DERs) and interconnected customers that operate jointly and continuously [1]. The implementation of these microgrids has increased in response to the growing energy demand and as an alternative to mitigate climate change, especially through the use of Renewable Energy Sources (RESs) [2]. Among these sources, photovoltaic solar, wind, and hydroelectric energy stand out. In particular, hydroelectric energy is one of the main sources used in Peru, with an installed capacity exceeding 69,445 MW, surpassing thermoelectric plants [3].

The increase in demand suggests the development of a solution that allows the simultaneous operation of different sources to meet the energy requirement. Based on this need, the use of a synchronizer is proposed, whose function is to minimize the differences in voltage, phase angle, and frequency between a generator and an active grid or an isolated source. This process is essential to avoid oscillations and prevent the deterioration of both the electrical and mechanical systems of the generator [1]. In electrical systems,

a synchronizer's function is to minimize voltage, phase angle, and frequency differences between a generator and an active grid or an isolated source. This process is essential to avoid oscillations and prevent the deterioration of both the electrical and mechanical systems of the generator [1]. In this context, this research aims to analyze the performance of a proposed soft synchronizer [4] and evaluate its effect on a salient pole synchronous generator driven by a hydraulic turbine [5]. Considering that although there is precedent regarding the modeling and simulation of synchronizers and generators, their joint application to a large-scale hydraulic turbine has not yet been addressed.

## 2. State of the Art

This section details studies conducted on reference frame transformation for three-phase sources, soft synchronization techniques for coupling two three-phase sources, and the operation of a Francis-type hydraulic turbine generator. The scientific paper "A New Method for Three-phase Voltage Detection and Protection Based on Reference Frame Transformation" proposes the use of reference frame transformation for a three-phase source that, in phasor form,



is in a stationary axis. By performing this transformation, the system transitions to a rotating two-phase frame using a transformation known as “Park’s Transformation.” Once the transform values are obtained, the voltage magnitude of phase a is calculated. This article employs the transformation for three-phase voltage detection and protection, allowing the method to respond immediately to voltage faults in the grid. Without this transformation, calculations take longer and delay response to voltage faults [6].

Another scientific paper, “New Ideas for a Soft Synchronizer Applied to CHP Cogeneration,” also employs this reference frame transformation. However, in this case, it not only calculates the voltage magnitude but also the phase angle of phase a, enabling soft synchronization between an electrical system and a 460 V diesel synchronous generator.

Additionally, a signal conditioner is implemented to compensate for variations in system voltage and phase angles, and these variations can cause an imbalance in the system, preventing the transformation from correctly calculating magnitude and angle. The synchronizer includes an exact timing calculation for when both systems reach the same angle, considering breaker closure time and linear slip frequency. A rule-based controller is used for speed and voltage adjustment [4].

The effect of faults in the electrical network, disturbances, harmonics, and notches is addressed in [6], where different algorithms are used to perform the synchronization (adaptive filter, Zero Crossing method, filter based on dq and  $\alpha\beta$  transformations, as well as an adaptive PLL), the latter being optimal to adapt the system to applications with photovoltaic systems or hydraulic turbines, its limitation being the complexity of the algorithm.

A synchronization model for a micro-hydroelectric power plant and a diesel generator is presented in [7], which simulates the joint operation of the system under variable loads. It is observed that the deviation value during synchronization is lower, achieving a speed within the permissible range. However, the limiting factor in the simulation is the speed control, which affects the transient response by being set at 1 pu. After conducting an extensive review of the research topic, it can be concluded that the reference frame transformation, known as Park’s Transformation, is divided into two stages:

- A matrix that converts the three-phase system into a two-phase system, known as Clarke’s Transformation.
- A matrix that converts the stationary reference frame into a rotating reference frame.

In the article “New Ideas for a Soft Synchronizer Applied to CHP Cogeneration”, it is observed that the Clarke’s Transformation matrix used is incorrect, as the signs in the

second row vary. Additionally, the article employs a rotation matrix that aligns phase a of the three-phase system with the d-axis of the transformation. However, it is essential to use a matrix that aligns phase **a** with the **q**-axis, as this ensures the correct calculation of the phase a angle in the three-phase system. This assertion is verified through simulations using the Park transformation equations and the transformation blocks in Simulink within MATLAB. The results conclude that the article presents discrepancies between its theoretical equations and its Simulink simulations.

## 2.1. Literature Gap and Contribution of the Study

After a detailed analysis of the literature, the following gaps have been identified:

### 2.1.1. Discrepancies in Park’s Transformation

- In [4], discrepancies are observed between the theoretical equations and the Simulink simulations. Additionally, the Clarke transformation matrix used is incorrect, as the signs in the second row vary.
- The impact of these errors on the synchronization and protection of three-phase systems has not been thoroughly validated.

### 2.1.2. Limitations in Generator Synchronization

- The synchronization method in [4] is based on a rule-based controller but does not optimize the compensation for variations in voltages and phase angles.
- In [6], the synchronization model does not address the effect of load variations or the influence of improved controller tuning during the transient period.

## 2.2. Innovation and Contribution of This Study

### 2.2.1. Correction and Validation of Transformations

- Discrepancies in Park’s Transformation will be analyzed, and a corrected version will be proposed to ensure the proper alignment of phase a with the q-axis.
- The Clarke transformation matrix used in previous studies will be compared with the correct version, evaluating its impact on voltage and phase angle measurements.

### 2.2.2. Optimization of the Synchronization Process

- A more robust controller will be designed for synchronization between electrical systems and Francis’s turbine generators, improving transient response and reducing deviations.
- An analysis and simulation of the main characteristic magnitudes of the soft synchronizer proposed for applications in hydroelectric plants in conjunction with an electrical grid, will be carried out.

## 2.3. Differences from Previous Studies

Unlike the reviewed articles, this study focuses on mathematically and computationally validating reference transformations for synchronization optimization and

evaluating their performance based on applications in medium- and high-voltage networks.

### 3. Theoretical foundation

To perform synchronization, a method is needed that can measure a three-phase system in a simple way to begin parallel operation. The method described in this section is the Park's Transform [4, 6, 9, 10]. This simple but efficient method consists of a reference frame transformation that can measure a three-phase AC source as if it were a DC source, thus allowing the verification of synchronization criteria. In Fig. 1, the three-phase source expressed in phasor form ( $V_a, V_b, V_c$ ) can be transformed to a two-phase system ( $V^\alpha, V^\beta$ ) on an orthogonal stationary axis ( $\alpha, \beta$ ) by means of the reference frame transformation, this transform is known as Clarke's Transform.

$$\begin{bmatrix} V^\alpha \\ V^\beta \end{bmatrix} = \frac{2}{3} \begin{bmatrix} 1 & -\frac{1}{2} & -\frac{1}{2} \\ 0 & \frac{\sqrt{3}}{2} & -\frac{\sqrt{3}}{2} \end{bmatrix} \begin{bmatrix} V_a \\ V_b \\ V_c \end{bmatrix} \quad (1)$$

Now, if the stationary axis ( $\alpha, \beta$ ) is projected onto the rotating axes ( $d, q$ ), which rotate at a speed  $\omega_r$ , as shown in Figure 2. The relationship between the stationary axis and the rotating axis for a q-axis alignment with phase a can be described as:

$$\begin{bmatrix} V^d \\ V^q \end{bmatrix} = \begin{bmatrix} \sin \theta_r & -\cos \theta_r \\ \cos \theta_r & \sin \theta_r \end{bmatrix} \begin{bmatrix} V^\alpha \\ V^\beta \end{bmatrix} \quad (2)$$

The three-phase variables rotate at a speed  $\omega$  when observed in a stationary reference frame. However, if they are transformed into a rotating reference frame at a speed  $\omega_r$  and assuming  $\omega = \omega_r$ , they will appear to be stationary in the rotating frame. In other words, they can be considered as Direct Current (DC) variables. Using this method, it is possible to control alternating current machines easily, as if they were direct current machines. If Equations (1) and (2) are combined, the transformation would be described by the following equation:

$$\begin{bmatrix} V^d \\ V^q \end{bmatrix} = \frac{2}{3} \begin{bmatrix} \sin \theta_r & \sin \left( \theta_r - \frac{2\pi}{3} \right) & \sin \left( \theta_r + \frac{2\pi}{3} \right) \\ \cos \theta_r & \cos \left( \theta_r - \frac{2\pi}{3} \right) & \cos \left( \theta_r + \frac{2\pi}{3} \right) \end{bmatrix} \begin{bmatrix} V_a \\ V_b \\ V_c \end{bmatrix} \quad (3)$$

Where the  $V^d$  and  $V^q$  axes rotate at a speed  $\omega_r$  so the angle between the stationary and rotating reference frames is defined by the following equation:

$$\theta_r = \int_0^t \omega_r(\tau) d\tau + \theta_r(0) \quad (4)$$

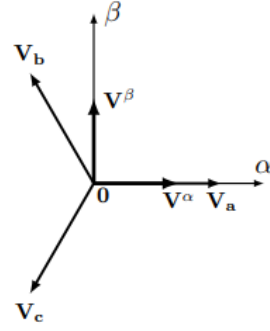


Fig.1. Transformation A-B-C to coordinates  $\alpha y \beta$

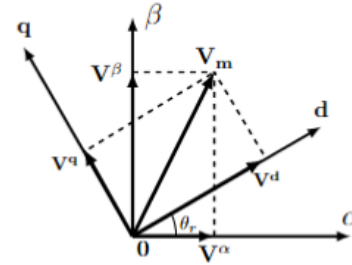


Fig. 2. Transformation  $\alpha y \beta$  to coordinates d-q

The transformation expressed in Equation (3) is known as Park's Transform and is used in calculations for three-phase electrical machines. For this article, this transformation is carried out for an alignment of the a phase with the q axis [10]. The choice of this alignment allows us to calculate the magnitude and angle so that it is consistent with Matlab simulations.

The Park transformation is then applied to a three-phase signal.

$$\begin{bmatrix} V_a \\ V_b \\ V_c \end{bmatrix} = \begin{bmatrix} V_m \sin(\omega t + \varphi) \\ V_m \sin(\omega t + \varphi - 120^\circ) \\ V_m \sin(\omega t + \varphi + 120^\circ) \end{bmatrix} \quad (5)$$

Substituting into equation (1)

$$\begin{bmatrix} V^\alpha \\ V^\beta \end{bmatrix} = \begin{bmatrix} V_m \sin(\omega t + \varphi) \\ -V_m \cos(\omega t + \varphi) \end{bmatrix} \quad (6)$$

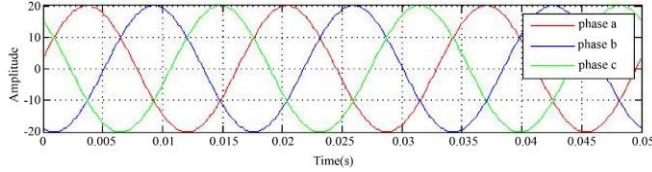
And substituting these values into equation (2) and considering  $\theta_r = \omega t$

$$\begin{bmatrix} V^d \\ V^q \end{bmatrix} = \begin{bmatrix} V_m \cos \varphi \\ V_m \sin \varphi \end{bmatrix} \quad (7)$$

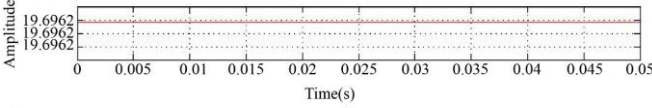
The Park transformation is used to calculate the magnitude (Mag) and the angle of the original signal for phase a, as follows:

$$Mag = \sqrt{(V^d)^2 + (V^q)^2} = V_m \quad (8)$$

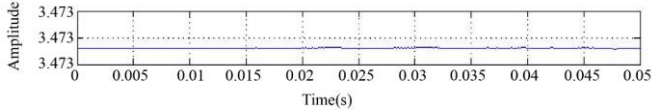
$$Angle = \tan^{-1}\left(\frac{V^q}{V^d}\right) = \varphi \quad (9)$$



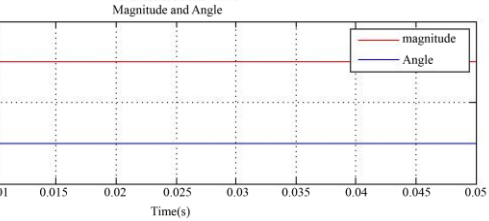
(a) Three-phase signal



(b) components  $V^d, V^q$



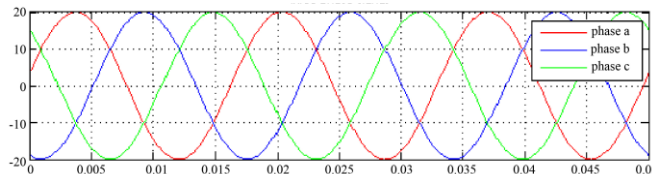
(c) magnitude and angle



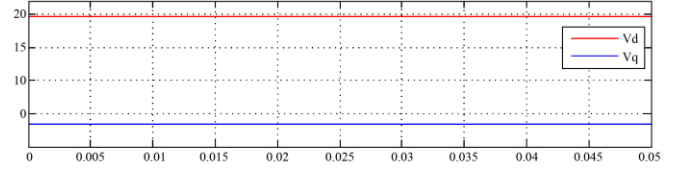
(c) magnitude and angle  
Fig. 3 Simulation for programming

The Park transformation is now simulated by developing a program with these equations in MATLAB, as well as by using the Park block in Simulink, whose results must match. In Figure 3(a), a three-phase source with a magnitude of 20V and a phase angle of  $10^\circ$  for phase a is shown. In Figure 3(b), we see the Park transformation applied through the  $V^d, V^q$  components calculated from equation (3), and as can be verified, both are DC signals. In Figure 3(c) shows the magnitude and angle calculated from equations (8) and (9), which, as expected, match the magnitude and angle of phase a of the three-phase source.

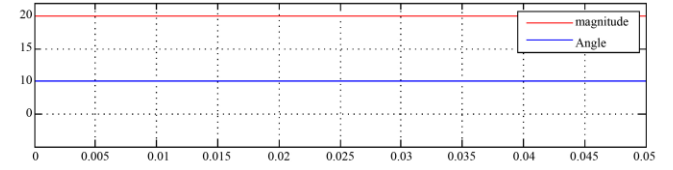
In Figure 4, the simulation of Park's transformation using Simulink blocks is presented. Figure 4(a) shows the three-phase signal. Figure 4(b) shows the  $V^d, V^q$  components, and Figure 4(c) shows the magnitude and angle. As can be seen, the values match those obtained using the mathematical equations.



(a) three-phase signal



(b) components  $V^d, V^q$



(c) magnitude and angle

Fig. 4 Simulink block simulation

### 3.1. Signal Conditioner

For the correct functioning of the algorithm described in the previous section, it must be taken into account that the original signals may have a small imbalance, since the excessive imbalance is protected by a system that prevents the operation of the generator circuit breaker. These small imbalances cause an oscillation in the calculations made (magnitude and angle). This small amount of imbalance must be regulated in the source signal for the correct operation of the synchronizer. In this article, a signal conditioner is included before applying the reference frame transformation. In the signal conditioning block, it converts unbalanced signals into three-phase symmetrical virtual signals. As a result, a more accurate measurement of the phase angle can be obtained for the original signals containing small imbalances. Below, a brief explanation of how to obtain these virtual signals will be developed through the following mathematical equations.

In [15], three coplanar vectors can be expressed in terms of three new vectors using three simultaneous linear equations with constant coefficients. Additionally, a unique symmetric solution exists, which can be expressed by the following equations:

$$V_a = V_1 + V_2 + V_0 \quad (10)$$

$$V_b = a^2V_1 + aV_2 + V_0 \quad (11)$$

$$V_c = aV_1 + a^2V_2 + V_0 \quad (12)$$

Where  $a = e^{j\frac{2\pi}{3}}$  is a phasor operator defined to rotate a phasor vector forward by  $120^\circ$  [9]. Solving the system

$$V_0 = \frac{1}{3}(V_a + V_b + V_c) \quad (13)$$

$$V_1 = \frac{1}{3}(V_a + aV_b + a^2V_c) \quad (14)$$

$$V_2 = \frac{1}{3}(V_a + a^2V_b + aV_c) \quad (15)$$

These solutions provide the vectors  $V_0$  for the zero-sequence,  $V_1$  for the positive-sequence, and  $V_2$  for the negative-sequence. Using the solution for the positive sequence:

$$\begin{bmatrix} \tilde{v}_a \\ \tilde{v}_b \\ \tilde{v}_c \end{bmatrix} = \begin{bmatrix} 1 \\ a^2 \\ a \end{bmatrix} V_1 \quad (16)$$

Virtual signals created using a positive sequence have average effects on the original signals in aspects of magnitude and phase.

Figure 5(a) shows the imbalance caused by the magnitude asymmetry of phase c, and there is also an angle asymmetry of phase b. If the magnitude or angle of a phase changes, the three-phase system is unbalanced. We solve this imbalance using equations (14) and (16) by creating virtual three-phase signals that are balanced and have the average magnitude and phase of the original signals (Figure 5(c)).

Figure 5(a) shows the time domain simulation of the magnitude and angle asymmetry case. Although the magnitude of one phase c has been reduced to 85%, the magnitude of the three-phase voltages after the signal conditioner has been reduced to 93%, but still maintains balance.

In the case of changing the phase angle b by 10 degrees, the phase angle of the entire created virtual system has changed slightly, but not significantly. In Figures 5(b) and 5(d), we observe the magnitude and angle calculated using the Park's transform.

The results obtained in Figure 5(b) are from the original unbalanced system, and as we see, they have oscillations in both magnitude and angle. On the other hand, the measurement results on the signals after the conditioner, Figure 5(d), are stable and consistent.

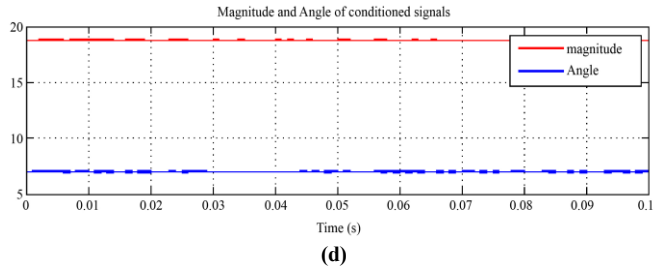
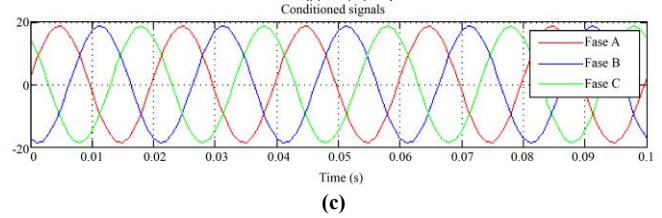
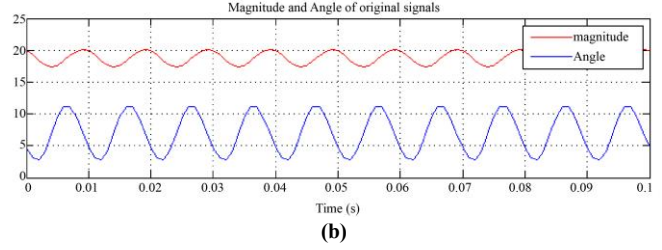
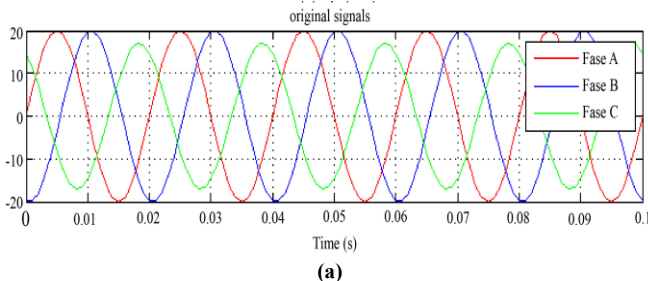


Fig. 5(a) Unbalanced system, (b) Magnitude and phase of the unbalanced system, (c) Balanced system, and (d) Magnitude and phase of the balanced system.

#### 4. Modeling and Simulation

This section includes the main models used for simulation in the Matlab Simulink environment, which, although it includes non-linear elements that improve accuracy compared to a real system, it is not possible to recognize other effects such as ripple and noise of the electrical system as well as hysteresis effects and environmental effects that alter the operation of the equipment, such as temperature and relative humidity.

The simulation of the synchronization process of the power grid and the hydro turbine generator is performed based on the Specialized Power Systems library, a subcategory of the Simscape Electrical library [11]. Then a breaker is introduced, shown in its closed condition, connected to the 13.8 kV/220 kV transformer, whose output is connected to the 150 MW reference load. As well as the connection to the transformer, a circuit breaker is used for parallel operation with the hydro generator.

The circuit breaker closure is controlled by the synchronizer (com), which in turn will adjust the voltage and speed of the turbine in such a way that the following criteria are met: slip frequency  $F_s \leq 0.1\text{Hz}$ , phase difference  $\theta_s \leq 1^\circ$ , and voltage variation  $\Delta V \leq 3\%$ .

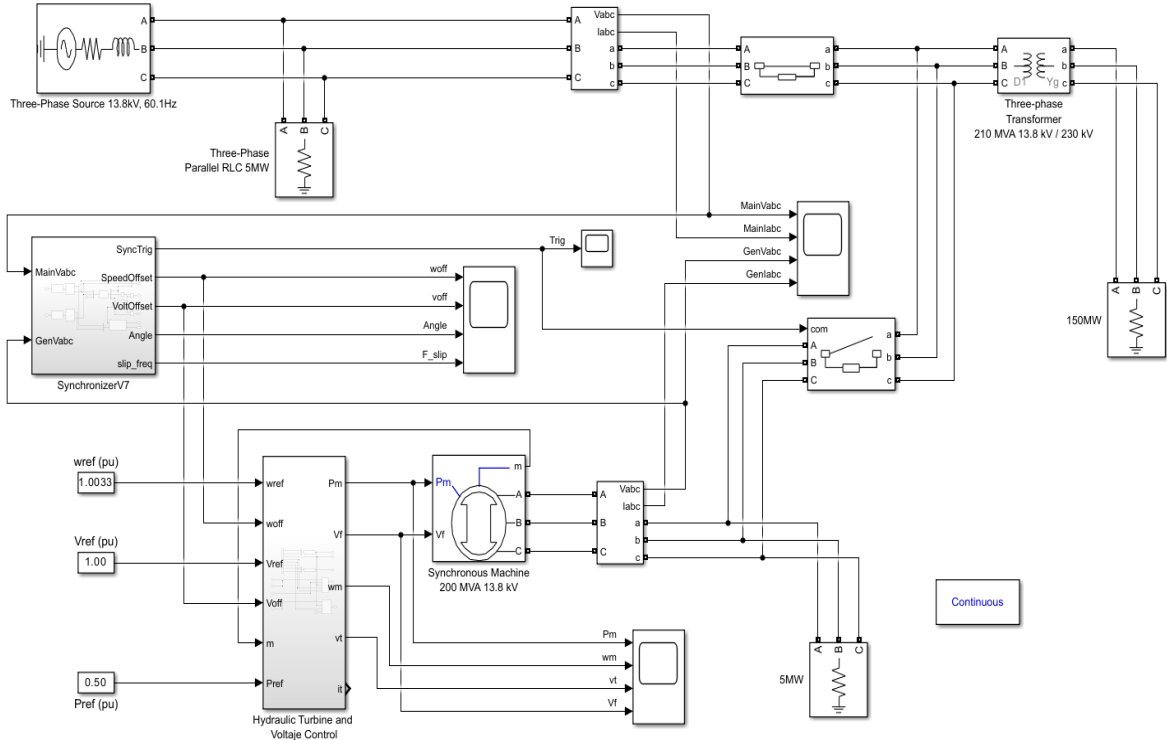


Fig. 6 Block diagram-HTG-EPS synchronization

4.1. Power Generation System

The synchronous salient pole generator shown in Figure 6 is based on the “Synchronous Machine Pu Standard” block found in reference [12] in model 2.1, and this is based on the IEEE 1110-2002 standard represented in Figure 7 [13].

The 200 MW generator model used comes from [5] and [14], and the generator reference values (reactance, time constants, inertia coefficients, and nominal values) are taken according to Table 1. The initial conditions will be taken from the steady state of the system for a reference voltage and speed coming from the excitation system and the governor, respectively.

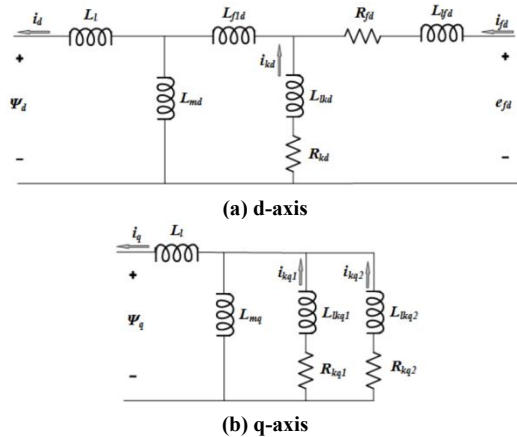


Fig. 7 Equivalent circuit - salient pole generator

4.2. Hydraulic Turbine and Voltage Controller

The block in Figure 8 represents the operation of the excitation system and an Hydraulic Turbine and Governor (HTG) block, which will receive the reference voltage, speed and power ‘Vref’, ‘wref’ and ‘Pref’ as inputs and then have as output the excitation voltage ‘Vf’ and the mechanical power ‘Pm’, which are inputs to the generator block. Also included are the ‘woff’ and ‘voff’ inputs, which represent the speed and voltage required by the synchronizer. Also note that the upper part shows as output the positive sequence terminal voltage ‘Vt’, which will be used as a reference for measuring the magnitude of the generator’s ac output voltage. ‘wref’ and ‘Vref’ are represented as constants in Figure 4 and are 1.0033 and 1.00 pu (60.2 Hz and 13.8 kV) such that the initial slip frequency of 0.1 Hz with respect to the main source is produced.

Table 1. Synchronous generator parameters

Parameter	Unit	Value
Nominal power, line-to-line voltage, frequency	Pn(VA) Vn(Vrms) fn(Hz)	200e6 13.8e3 60
Reactances	Xd (pu)	1.305
	Xd' (pu)	0.296
	Xd'' (pu)	0.252
	Xq (pu)	0.474
	Xq' (pu)	0.243
Xl (pu)		0.18
Time Constants	Td' (s)	1.01

	Td'' (s)	0.053
	Tqo'' (s)	0.1
Stator Resistance	Rs (pu)	2.8544e-3
Inertia coefficient	H(s)	3.2
friction factor	F(pu)	0
pole pairs	p()	8

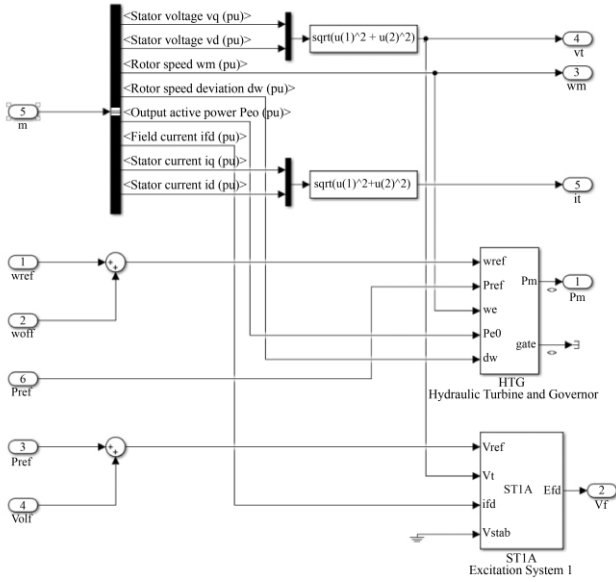


Fig. 8 Hydraulic turbine and voltage controller

4.2.1. Hydraulic Turbine and Governor

This block is responsible for regulating the generator speed (frequency and phase) for different loads. The Simulink block is based on the governor model of reference [15] with a compensation (droop reference) that can depend on the difference with respect to the reference power or the water inlet opening level, as shown in Figure 7 [15]. Figures 8 [15] and 9 [15] represent the non-linear model of the hydraulic turbine and the servo, respectively. The first model represents a control system that has as input the servo opening level and as output the mechanical power, which enters the synchronous generator.

Table 2. Hydraulic turbine and governor parameters

Parameter	Unit	Value
Servo-motor	Ka()	10/3
	Ta(sec)	0.07
Gate opening limits	gmin (pu)	0.01
	gmax(pu)	0.9751
	vgmin (pu/s)	-0.5
	vgmax(pu/s)	0.5
Permanent droop and regulator	Rp()	0.0
	Kp()	1.91
	Ki()	0.215
	Kd()	0
	Td(s)	0.01
Hydraulic turbine	beta()	0.00
	Tw(sec)	2.67

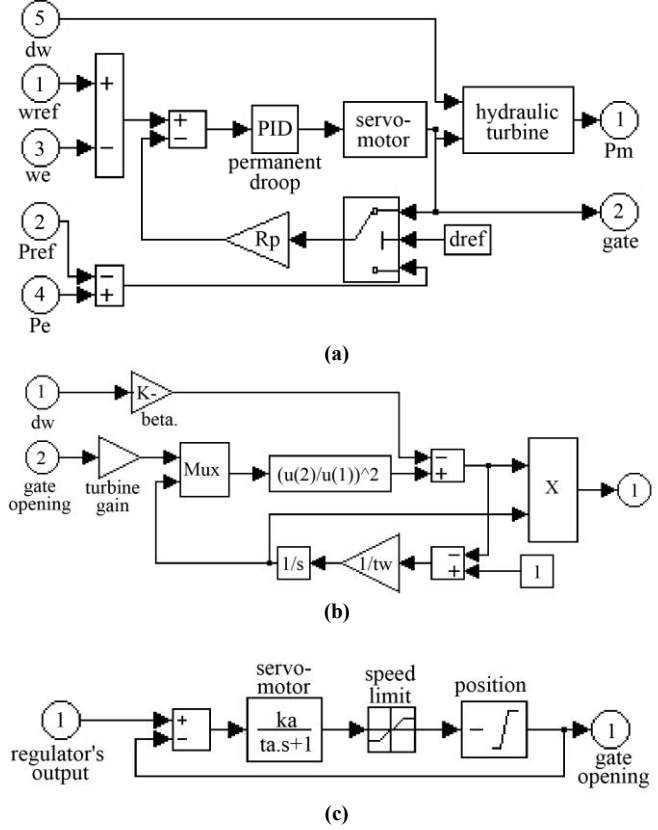


Fig. 9(a) Hydraulic system governor, (b) Hydraulic turbine, and (c) Servo.

On the other hand, the servomotor is represented by a first-order function, which, by including an integrator block and a feedback loop, represents a second-order function. The PID controller parameters associated with the turbine governor, such as the servo time constants, the Kp, Ki, and Kd constants, and the saturation limits, were taken from Table 2. [5, 14].

4.2.2. Excitation System

This system is responsible for generating the excitation voltage of the generator. The block diagram in Figure 10 represents a simplified model of the EFD excitation system, ST1C [16]. It has a lead-lag compensator, a voltage regulator, a voltage-dependent damping function, an exciter, and an input stage saturation block, and an output of the exciter according to the parameters in Table 3.

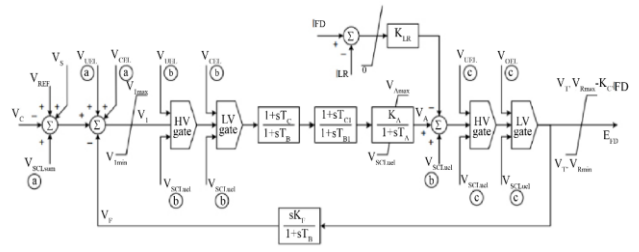


Fig. 10 Excitation system model ST1C

**Table 3. Parameters of the excitation system model STIC**

Parameter	Unit	Value
Low-pass filter time constant	Tr(s)	20e-3
Voltage regulator gain and time constant	Ka	150
	Ta(s)	0.01
Voltage regulator output limits	VRmin(pu)	-6.0
	VRmax(pu)	6.43
Damping filter gain and time constant	Kf	0.001
	Tf(s)	0.001
Transient gain reduction lead and lag time constants	Tb(s)	0.3
	Tc(s)	0.025
	Tb1(s)	0.05
	Tc1(s)	0.02
Exciter output current limiter gain	KLR(pu)	1
Exciter output current limit reference	ILR(pu)	2
Rectifier loading factor	Kc(pu)	0.038

### 4.3. Soft Synchronizer

Figure 11 shows the soft synchronizer. The voltage input signals from the EPS (MainVabc) and the Synchronous Generator (GenVabc) pass through a signal conditioner where the signal averaging will be applied and the virtual output signals will be generated, which will enter the magnitude and phase detector, which includes the  $\alpha\beta$  and  $dq$  transformations to obtain the voltage and phase magnitudes. The outputs are directed to the SyncCtrl block that will regulate the offset output speed to maintain the slip frequency of  $\pm 0.1$ Hz, as well as the offset voltage regulation to match that indicated by the main source with  $\pm 1\%$ . The Synchro function calculates the projected slip frequency for a delay of the complete closing of the breaker, represented by a Transport Delay block (Delay\_Trig), so that the  $0^\circ$  phase shift coincides with the closing of the breaker. An additional  $t_{step}$  transient\_time is included so that the closing function occurs after a certain time.

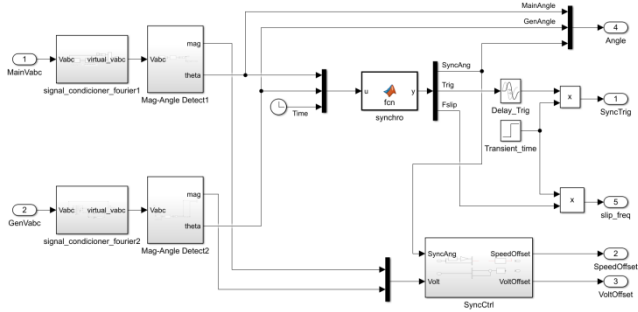
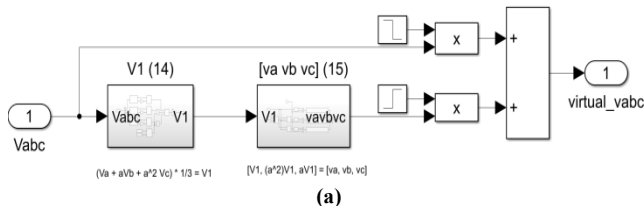
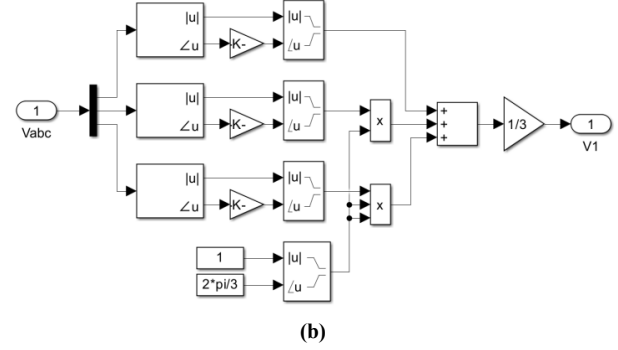


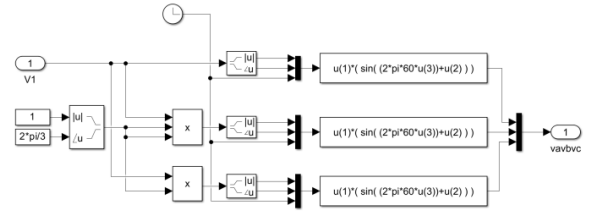
**Fig. 11 Soft synchronizer**



**(a)**



**(b)**



**(c)**

**Fig. 12(a) Signal conditioner, (b) Average signal, and (c) Obtaining virtual signals.**

#### 4.3.1. Signal Conditioner

The signal conditioner (signal\_conditioner\_fourier) of Figure 12. a performs the conversion of each signal to an amplitude and phase spectrum by applying the Fourier transform from the fundamental frequency of 60Hz. Equations (14) and (16) are applied to obtain the average signal and phase shift, calculated to obtain virtual signals  $\hat{v}_a$ ,  $\hat{v}_b$  y  $\hat{v}_c$  represented in Figures 12.b and 12.c, respectively, which will enter the magnitude and phase detection block.

#### 4.3.2. Magnitude and Phase Detection

Figure 13. a shows the representation of the Clarke and Clarke-Park transformations (Fig. 13.b and 13.c) to obtain  $\alpha\beta$  y  $dq$  applying the equations (1) and (2), respectively, including an  $\theta_{elec}$  equal to  $\omega t$  or  $2\pi f t$ . The transformations are performed on the virtual signals coming from the signal conditioner. Finally, the conversion of Cartesian to polar coordinates is performed according to equations (8) and (9) to obtain the angle in sexagesimal degrees and the magnitude in pu.

#### 4.3.3. Offset Voltage and Speed Controller

To obtain the offset speed and voltage required to reach the synchronization criterion, a PI controller is used, and for the offset speed, a rule-based controller or a PID controller can be used, as shown in Figure 14.

To obtain the proportional, integral, and derivative gains (for speed adjustment), tuning can be applied using the Ziegler-Nichols method. The simulation starts from the generator's steady state, where the synchronization criterion with respect to the slip frequency is met, so the controller will have no significant effect.

4.3.4. Obtaining the Circuit Breaker Closing Signal

The ‘synchro’ block in Figure 13 represents the function that would predict the value of the phase difference from obtaining the slope. The slip frequency is calculated from (18), and the future phase difference is calculated from (17), where  $\theta_k$  indicates the current phase difference,  $\theta_{k-1}$  the previously recorded phase difference value, and  $T_{bd}$  the circuit breaker closing time.

$$\hat{\theta} = \theta_k + T_{bd}(\theta_k - \theta_{k-1})/\Delta t \quad (17)$$

$$F_{slip} = \frac{\omega_s}{2\pi} = \frac{1}{2\pi} \frac{\partial \theta_s}{\partial t} \quad (18)$$

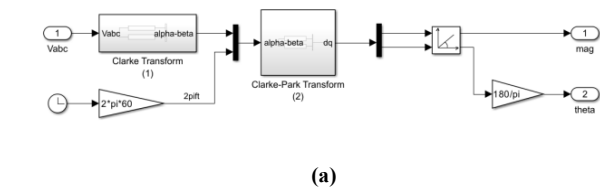
In this way, when the phase synchronization criteria ( $\hat{\theta}$ ) predicted less than  $1^\circ$  and slip frequency ( $F_{slip}$ ) less than 0.1 Hz are met, the ‘Trig’ output will change to 1, representing the closing of the circuit breaker so that the three-phase source and the generator operate simultaneously.

4.4. Traditional Synchronizer

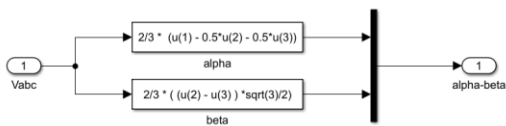
To simulate a traditional synchronizer, we will start from a case of simulating it for a window of  $\pm\theta_w$  as shown in Figure 15. From the eq. (19) we will calculate the dwell-time by estimating the time that should remain in the window based on the slip frequency  $F_s$  that exists between the main source and the generator. We will also predict the phase angle at the instant of the circuit breaker closing based on the circuit breaker closing time [17] according to equation (20). With this data, we will proceed to change the closing condition when the phase difference is  $\theta_{wc}$ . In the same way, the ‘Delay\_trig’ time of the synchronizer in Figure 13 [17] will be increased by the value of the calculated dwell-time.

$$dwell - time = \frac{2\theta_w}{360^\circ} F_s \quad (19)$$

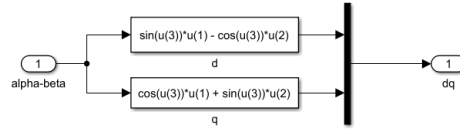
$$\theta_{wc} = \theta_w + T_{bd}(F_s)(360^\circ) \quad (20)$$



(a)



(b)



(c)

Fig. 13(a) Magnitude and phase detection, (b) Clarke Transformation, and (c) Clarke-Park transformation.

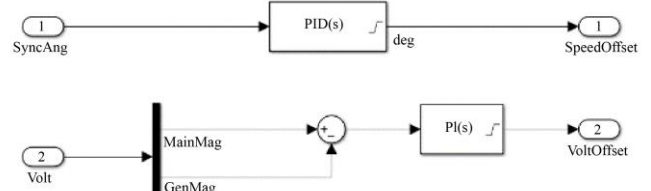


Fig. 14 Voltage and speed regulator

5. Results

The comparison of the operation corresponding to the traditional synchronizer based on dwell-time as explained in section 4.4 was carried out, and then the simulation of the soft synchronizer developed in section 4.3 was included.

For the first case, a window of  $\pm 10^\circ$  was considered, in addition to the 0.1 Hz slip frequency of the generator with respect to the electrical network. It is calculated that the maximum corresponding dwell time would be 0.55 s. Additionally, the phase shift for the breaker closing time of 0.058 s will be  $2.09^\circ$ . Then the breaker will close completely when there is a phase shift of  $12.09^\circ$ .

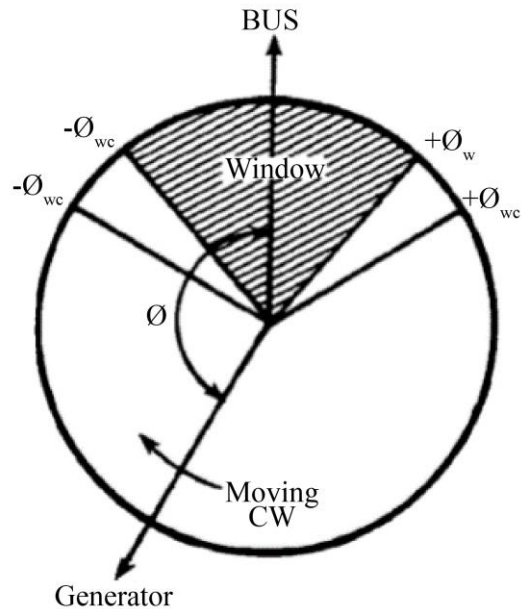


Fig. 15 Traditional synchronizer

However, in Figure 16.a the value of the circuit breaker closing angle varies slightly up to  $9.08^\circ$ , generating in the same way oscillations as those indicated in Figures 16.b, 16.c, 16.d, 16.e of the magnitudes of Mechanical Power (Pm), Terminal Voltage (Vt), Angular velocity ( $\omega$ ), and current Iabc respectively in pu. At  $t = 1.2s$ , when the circuit breaker closes, a sudden change in the previously mentioned magnitudes is observed. This can cause internal damage to the generator by exceeding the nominal current value, as shown in Figure 16.e. Likewise, in Figure 16.d, harmonics are observed in the voltage magnitude during and after synchronization.

Regarding the soft synchronizer in Figure 17, a difference is clearly observed, since the closure occurs at the exact moment that the circuit breaker closes completely,  $t = 0.82s$ , as indicated in Figure 17.a, significantly reducing the oscillations generated by the phase shift compared to the traditional synchronizer (Figure 17.b), as well as in harmonics (Figure 17.d) and the maximum current peak during synchronization (Figure 16.e). For both cases, the final speed values tend to be the same when operating in parallel and equal to the frequency of the active network (Figure 17.c).

Table 4 shows a summary of the percentage values of maximum overshoot with respect to the nominal value for both cases with respect to the magnitudes of voltage, power, and angular velocity with respect to Figures 16 and 17, where the improvement of the proposed system over a traditional one is clearly evident.

### 6. Discussion

A notable improvement is observed in the application of the soft synchronizer compared to the performance of a traditional synchronizer in the hydraulic turbine when comparing the variation with respect to the pu value.

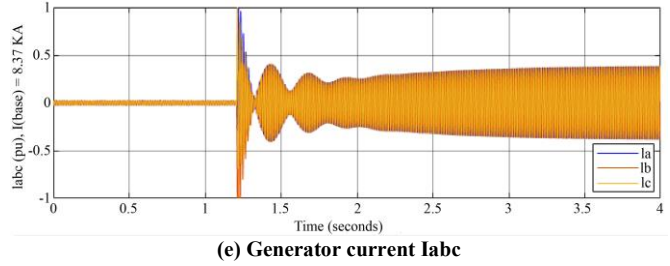
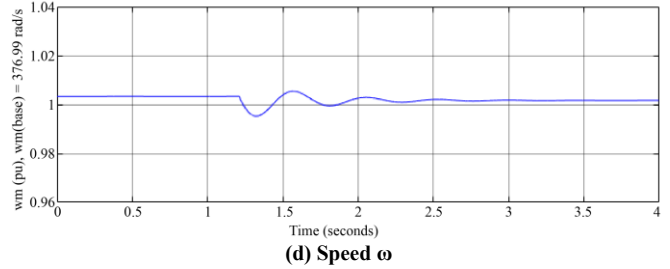
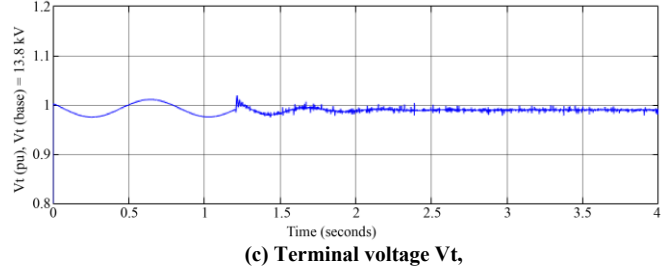
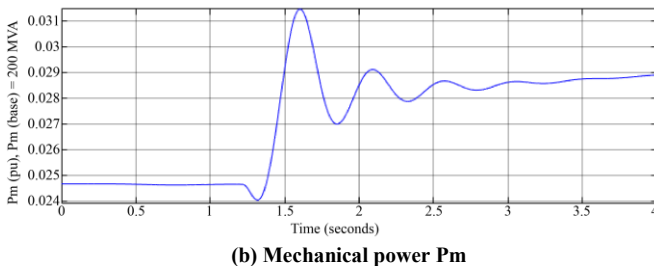
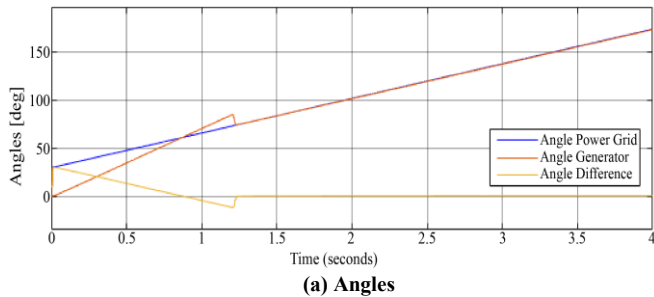
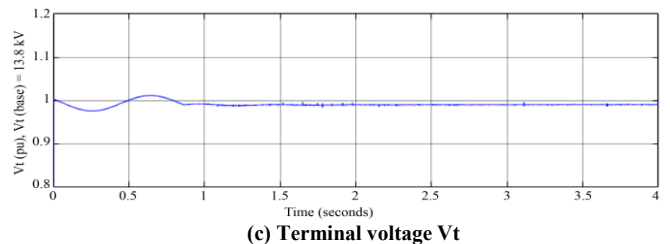
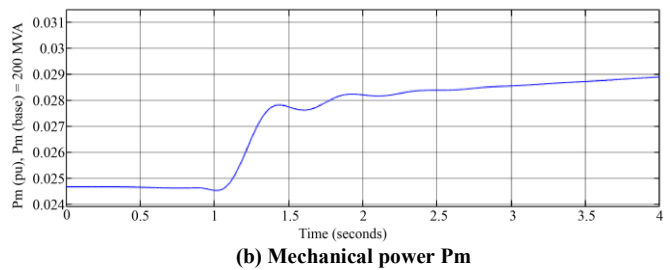
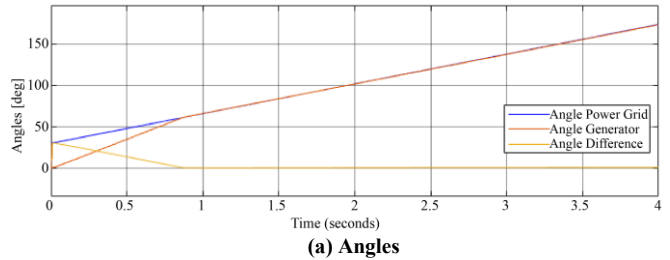


Fig. 16 Time response of traditional synchronizer



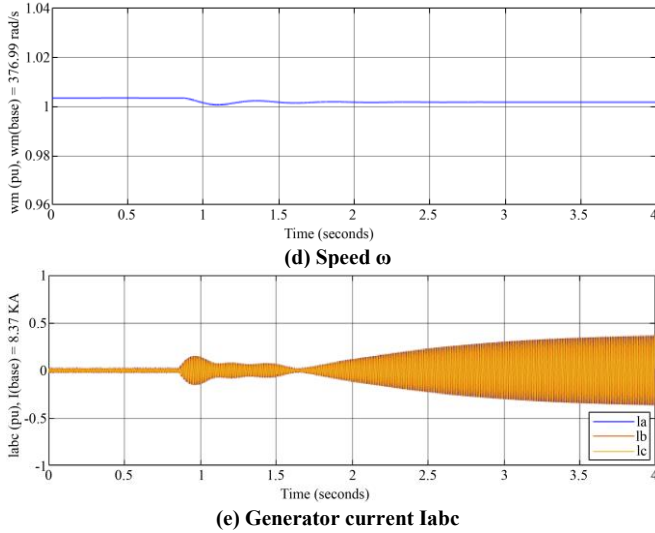


Fig. 17 Time response of soft synchronizer

However, both models used are based on the generator operating under optimal conditions according to the design conditions, such as reactances, and may be susceptible to changes in the mechanical model in a real application. However, the algorithm does not take into account the variables and parameters associated with the generator's own mathematical model, which indirectly affects the result by taking as reference the ripple, noise, and fluctuations in the voltage and current values typical of an implementation in a physical environment as well as in the electrical grid. For this purpose, it is essential to use filters in conjunction with the signal conditioner that operate without significantly altering the voltage measurement and affecting the phase determination. Unlike the synchronizers proposed in [4] and [7], it was applied in generators of higher power and voltage,

**References**

[1] Mobin Naderi et al., "Synchronization Stability of Interconnected Microgrids with Fully Inverter-based Distributed Energy Resources," *Journal of Modern Power Systems and Clean Energy*, vol. 11, no. 4, pp. 1257-1268, 2023. [CrossRef] [Google Scholar] [Publisher Link]

[2] Ritu Raj Shrivastwa et al., "Understanding Microgrids and Their Future Trends," *2019 IEEE International Conference on Industrial Technology (ICIT)*, Melbourne, VIC, Australia, pp. 1723-1728, 2019. [CrossRef] [Google Scholar] [Publisher Link]

[3] Ana Cecilia Moreno Alamo et al., "Study of Distributed Generation Systems that Supplies Electrical Energy to Distribution Networks," *2022 Portland International Conference on Management of Engineering and Technology (PICMET)*, Portland, OR, USA, pp. 1-13, 2022. [CrossRef] [Google Scholar] [Publisher Link]

[4] Changhee Cho et al., "New Ideas for a Soft Synchronizer Applied to CHP Cogeneration," *IEEE Transactions on Power Delivery*, vol. 26, no. 1, pp. 11-21, 2011. [CrossRef] [Google Scholar] [Publisher Link]

[5] Motilal Senapati, and Gyan Ranjan Biswal, "Dynamic Study of Salient Pole Synchronous Hydro Generator - Turbine Set Under Variable Excitation," *2015 Annual IEEE India Conference (INDICON)*, New Delhi, India, pp. 1-5, 2015. [CrossRef] [Google Scholar] [Publisher Link]

[6] Q. Zeng, and L. Chang, "A New Method for Three-Phase Voltage Detection and Protection Based on Reference Frame Transformation," *2004 IEEE 35th Annual Power Electronics Specialists Conference (IEEE Cat. No.04CH37551)*, Aachen, Germany, pp. 2489-2493, 2004. [CrossRef] [Google Scholar] [Publisher Link]

[7] S. P. Gawande et al., "Synchronization of Synchronous Generator and Induction Generator for Voltage & Frequency Stability Using STATCOM," *2010 3rd International Conference on Emerging Trends in Engineering and Technology*, Goa, India, pp. 407-412, 2010. [CrossRef] [Google Scholar] [Publisher Link]

allowing the development of new applications with other types of generators of renewable energy sources.

Table 4. Comparison between Soft Synchronizer and Traditional Synchronizer (Maximum Overshoots)

Magnitude	Traditional Synchronizer	Soft Synchronizer
Terminal Voltage	1.02%	0.22%
Mechanical Power	10.71%	0.36%
Rotor Speed	1.18%	0.27%

**7. Conclusion**

Through the simulation in Simulink of a hydraulic generator, the effect of soft synchronization was verified and validated by adjusting the moment of closing of the circuit breaker when there is the smallest difference in the phase angle and the synchronization criteria regarding voltage, phase, and frequency are met. Soft synchronization allows for to reduce of the oscillations of the generator variables, as well as the harmonics generated with traditional synchronization.

Although the main characteristic considered in this article was the phase adjustment, for a practical application, it is necessary to evaluate the characteristics addressed in the previous section regarding the generation system and the electrical grid.

**Acknowledgments**

The authors thank the Universidad Nacional de San Agustín de Arequipa for the support and knowledge to develop this research.

- [8] Adrian Timbus et al., "Synchronization Methods for Three Phase Distributed Power Generation Systems - An Overview and Evaluation," 2005 *IEEE 36th Power Electronics Specialists Conference*, Dresden, Germany, pp. 2474-2481, 2005. [[CrossRef](#)] [[Google Scholar](#)] [[Publisher Link](#)]
- [9] Edith Clarke, *Circuit Analysis of AC Power Systems, Symmetrical and Related Components*, vol. 1, New York, 1943. [[Google Scholar](#)]
- [10] Mathworks. Park's Transform, 2024. [Online]. Available: <https://la.mathworks.com/help/sps/ref/parktransform.html>
- [11] MathWorks, Simscape Electrical, 2024. [Online] Available: <https://www.mathworks.com/products/simscape-electrical.html>
- [12] "IEEE Guide for Synchronous Generator Modeling Practices and Applications in Power System Stability Analyses," *IEEE Power Engineering Society*, pp. 1-81, 2003. [[Google Scholar](#)] [[Publisher Link](#)]
- [13] Mathworks, Hydraulic Turbine and Governor, 2024. [Online]. Available: <https://la.mathworks.com/help/sps/powersys/ref/synchronouismachinefundamental.html>
- [14] Basile Kawkabani, Christophe Nicolet, and Alexander Schwery, "Modeling and Control of Large Salient-Pole Synchronous Hydro Generators and Stability Issues in Isolated Production Mode," 2013 *IEEE Workshop on Electrical Machines Design, Control and Diagnosis (WEMDCD)*, Paris, France, pp. 148-157, 2013. [[CrossRef](#)] [[Google Scholar](#)] [[Publisher Link](#)]
- [15] Working Group Prime Mover and Energy Supply, "Hydraulic Turbine and Turbine Control Models for System Dynamic Studies," *IEEE Transactions on Power Systems*, vol. 7, no. 1, pp. 167-179, 1992. [[CrossRef](#)] [[Google Scholar](#)] [[Publisher Link](#)]
- [16] "IEEE Recommended Practice for Excitation System Models for Power System Stability Studies," IEEE Std 421.5-2016, pp. 1-207, 2016. [[Google Scholar](#)] [[Publisher Link](#)]
- [17] Woodward Reference Manual, Governing Fundamentals and Power Managements, 2004. [Online]. Available: <https://www.pbm.hr/media/1101/woodward-governing-fundamentals.pdf>